

# Intrinsic surface plasmon-phonon polaritons: A non-perturbative quantum theory

D. Hagenmüller,<sup>1,2</sup> J. Schachenmayer,<sup>1,2</sup> C. Genet,<sup>1</sup> T. W. Ebbesen,<sup>1</sup> and G. Pupillo<sup>1,2</sup>

<sup>1</sup>*ISIS (UMR 7006) and icFRC, University of Strasbourg and CNRS, 67000 Strasbourg, France*

<sup>2</sup>*IPCMS (UMR 7504), University of Strasbourg and CNRS, 67000 Strasbourg, France*

(Dated: May 17, 2022)

We investigate light-matter coupling in metallic crystals where plasmons coexist with phonons exhibiting large oscillator strength. We demonstrate theoretically that this coexistence can lead to strong coupling without external resonators in certain materials. A non-perturbative self-consistent Hamiltonian method is presented that is valid for arbitrarily large phonon-photon coupling strengths, i.e., in the vibrational ultrastrong coupling regime. We show that phonons can be controlled by tuning the electron density and the crystal thickness. In particular, a low-energy dressed phonon with large wave vectors arises in the case of quasi-2D crystals, which can in principle lead to changes of key material properties such as the electron-phonon scattering.

PACS numbers: 42.50.Pq, 71.36.+c, 73.20.Mf, 78.68.+m

Surface plasmon polaritons (SPPs) are evanescent waves propagating along metal-dielectric interfaces, which originate from the coupling between light and collective electronic modes in metals, called plasmons [1]. Thanks to the confinement of light below the diffraction limit [2–7], plasmonic resonators allow for the exploitation of SPPs to engineer strong light-matter coupling [8–26]. This is usually achieved by placing quantum emitters (excitons or phonons) in a dielectric region near the metal surface. In this case, SPPs play the role of the photons in usual cavity-QED setups, which has opened the way to breakthrough applications in material science and chemistry [27–37] in the strong and even ultrastrong coupling regimes. The latter corresponds to situations where the light-matter coupling strength reaches a few percent of the relevant transition frequencies [38–40], which is now frequently achieved in experiments [41–54]. Interestingly, most quantized models are well suited to describe the strong coupling regime [20, 21, 55], while a corresponding theory for the ultrastrong coupling regime of SPPs is still missing.

Field quantization in dispersive media is a long-standing problem [56–75], which also arises in the context of phonon-photon interactions [76–80]. For instance, surface phonon polaritons stemming from the coupling between light and ionic charges typically occur in the reststrahlen band of polar crystals [81, 82]. Surface phonon and plasmon polaritons can not generally coexist due to the screening of the ion charges by electrons. Nevertheless, exceptions exist such as bilayer graphene [83], alkali-doped C<sub>60</sub> [84, 85], organic conductors such as K – TCNQ [86–88], as well as some transition metal compounds [89]. Whether the strong light-matter interactions stemming from the coexistence of plasmons and phonons with large oscillator strengths can affect the quantum properties of the crystal itself is an interesting prospect, which has remained unexplored.

In this work, we propose and investigate the possibility to tune material properties of certain crystals

via an hybridization of phonons, plasmons, and photons which is intrinsic to the material, i.e., without the use of an external resonator. We find that strong light-matter interactions within the crystal offer a unique possibility to control the phonon energy and momentum by tuning the electron density and the crystal thickness: A “dressed” low-energy phonon arises in the ultrastrong coupling regime, where the different coupling strengths become comparable to the phonon frequency. This dressed phonon is shown to exhibit unusually large momenta comparable to the Fermi wave vector in the case of quasi-2D crystals, which could therefore affect key material properties such as, e.g., the electron-phonon scattering. We provide realistic parameters showing that this situation may occur in bilayer graphene.

We utilize a self-consistent Hamiltonian method that is valid for all regimes of interactions between light and matter in the absence of dissipation. This approach is based on a generalization of that introduced by Todorov [90], and proceeds according to the following scheme: *i*) We diagonalize the matter Hamiltonian leading to plasmon-phonon hybridization in the crystal; *ii*) We derive the coupling Hamiltonian of the new hybrid modes to photonic degrees of freedom, which provides a functional relation between the field penetration depths and the surface mode frequencies; and *iii*) We determine these two latter parameters self-consistently as follows: Starting with a given surface mode frequency, we use the Helmholtz equation to compute the field penetration depths entering the Hamiltonian. The latter is diagonalized and the algorithm is repeated with the lowest eigenvalue as a new surface mode frequency, which is again used to construct a new Hamiltonian until convergence. Our method can be easily generalized to various geometries and surrounding media, and differs from the usual effective quantum description of strong coupling between excitons and quantized SPPs [20, 21]. We show in the supplemental material [91] that the latter model leads to unphysical behaviors in the ultrastrong coupling regime.

We consider a crystal of surface  $S$  and thickness  $\ell$  in air, featuring a long-wavelength plasmon mode with plasma frequency  $\omega_{\text{pl}}$  and an optical phonon mode with frequency  $\omega_0$ . Both plasmons and phonons are polarized in the directions  $\mathbf{u}_z$  and  $\mathbf{u}_{\parallel} = \mathbf{r}/r$  (Fig. 1). The Hamiltonian is derived in the Power-Zienau-Woolley (PZW) representation [92, 93], which ensures proper inclusion of all photon-mediated dipole-dipole interactions, and can be decomposed as  $H = H_{\text{pt}} + H_{\text{mat-pt}} + H_{\text{mat}}$ . The photon Hamiltonian reads  $H_{\text{pt}} = \frac{1}{2\epsilon_0} \int d\mathbf{R} \mathbf{D}^2(\mathbf{R}) + \frac{1}{2\epsilon_0 c^2} \int d\mathbf{R} \mathbf{H}^2(\mathbf{R})$ , with  $c$  the speed of light in vacuum,  $\mathbf{R} \equiv (\mathbf{r}, z)$  the 3D position, and  $\epsilon_0$  the vacuum permittivity. The light-matter coupling term is  $H_{\text{mat-pt}} = -\frac{1}{\epsilon_0} \int d\mathbf{R} \mathbf{P}(\mathbf{R}) \cdot \mathbf{D}(\mathbf{R})$ . Here,  $\mathbf{P} = \mathbf{P}_{\text{pl}} + \mathbf{P}_{\text{pn}}$  denotes the matter polarization field associated to the dipole moment density, where  $\mathbf{P}_{\text{pl}}$  and  $\mathbf{P}_{\text{pn}}$  correspond respectively to the plasmon and phonon contributions [94], and  $\mathbf{D}$  and  $\mathbf{H}$  are the displacement and magnetic fields associated to photonic degrees of freedom. The matter Hamiltonian  $H_{\text{mat}}$  consists of the free phonon and plasmon Hamiltonians, as well as a term  $H_{\text{p}^2} = \frac{1}{2\epsilon_0} \int d\mathbf{R} \mathbf{P}^2(\mathbf{R})$  containing the contributions of both plasmons and phonons  $\propto \mathbf{P}_{\text{pl}}^2, \mathbf{P}_{\text{ph}}^2$ , as well as a direct plasmon-phonon interaction  $\propto \mathbf{P}_{\text{pl}} \cdot \mathbf{P}_{\text{ph}}$ .

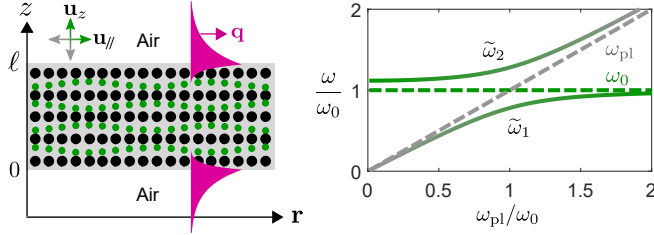


FIG. 1. Intrinsic surface plasmon-phonon polaritons: Metal of thickness  $\ell$  in air featuring a plasmon mode with frequency  $\omega_{\text{pl}}$  (gray dashed line) and an optical phonon mode with frequency  $\omega_0$  (green dashed line). Both plasmons and phonons are polarized in the directions  $\mathbf{u}_z$  and  $\mathbf{u}_{\parallel}$ . When  $\nu_{\text{pn}} \neq 0$  and  $\omega_{\text{pl}} \sim \omega_0$ , the matter Hamiltonian  $H_{\text{mat}}$  provides two hybrid plasmon-phonon modes with frequencies  $\tilde{\omega}_1$  and  $\tilde{\omega}_2$  [Eq. (1)] represented as a function of  $\omega_{\text{pl}}/\omega_0$  for  $\nu_{\text{pn}} = 0.5\omega_0$ . The surface polaritons generated by the coupling of these modes to light propagate along the two metal-dielectric interfaces with in-plane wave vector  $\mathbf{q}$ .

*i) Diagonalization of the matter Hamiltonian:* In order to first diagonalize  $H_{\text{mat}}$ ,  $\mathbf{P}_{\text{pn}}$  is written in terms of the bosonic phonon operators and is proportional to the ionic plasma frequency  $\nu_{\text{pn}} = \sqrt{\frac{Z^2 N}{M \epsilon_0 a^3}}$ , which plays the role of the phonon-photon coupling strength [91].  $N$  denotes the number of vibrating ions with effective mass  $M$  and charge  $Z$  in a unit cell of volume  $a^3$ . The plasmon polarization is provided by the dipolar description of the free electron gas [90] corresponding to that of the random-phase approximation [95] (RPA). In the long-wavelength regime,  $\mathbf{P}_{\text{pl}}$  is written in terms of bosonic

plasmon operators, superpositions of electron-hole excitations across the Fermi surface.  $H_{\text{mat}}$  can be put in the diagonal form  $H_{\text{mat}} = \sum_{\mathbf{Q}, \alpha, j=1,2} \hbar \tilde{\omega}_j \Pi_{\mathbf{Q}j\alpha}^\dagger \Pi_{\mathbf{Q}j\alpha}$  [91], where the hybrid plasmon-phonon annihilation and creation operators satisfy the bosonic commutation relation  $[\Pi_{\mathbf{Q}j\alpha}, \Pi_{\mathbf{Q}'j'\alpha'}^\dagger] = \delta_{\mathbf{Q}, \mathbf{Q}'} \delta_{j,j'} \delta_{\alpha,\alpha'}$ , and the hybrid mode frequencies [Fig. 1 b)] read:

$$2\tilde{\omega}_j^2 = \tilde{\omega}_0^2 + \omega_{\text{pl}}^2 \pm \sqrt{(\tilde{\omega}_0^2 - \omega_{\text{pl}}^2)^2 + 4\nu_{\text{pn}}^2 \omega_{\text{pl}}^2}. \quad (1)$$

Here,  $j = 1$  and  $j = 2$  refer respectively to the signs  $-$  and  $+$ , and the renormalized phonon square frequency  $\tilde{\omega}_0^2 = \omega_0^2 + \nu_{\text{pn}}^2$  is determined by the combination of the short-range restoring force related to the phonon resonance, and the long-range Coulomb force associated to the ion plasma frequency. The diagonalization procedure of  $H_{\text{mat}}$  further provides the transverse dielectric function of the crystal:

$$\epsilon_{\text{cr}}(\omega) = 1 - \frac{\omega_{\text{pl}}^2}{\omega^2} - \frac{\nu_{\text{pn}}^2}{\omega^2 - \omega_0^2}, \quad (2)$$

which was derived from a Green's function analysis in Ref. [81]. One can then use the eigenmodes basis of the matter Hamiltonian to express the total polarization field as:

$$\mathbf{P}(\mathbf{R}) = \sum_{\mathbf{Q}, \alpha, j} g_j \sqrt{\frac{\hbar \epsilon_0 \omega_{\text{pl}}^2}{2\tilde{\omega}_j V}} \left( \Pi_{-\mathbf{Q}j\alpha} + \Pi_{\mathbf{Q}j\alpha}^\dagger \right) e^{-i\mathbf{Q} \cdot \mathbf{R}} \mathbf{u}_\alpha, \quad (3)$$

with

$$g_j = \frac{\tilde{\omega}_j^2 \left( 1 + \nu_{\text{pn}}^2 / \omega_{\text{pl}}^2 \right) - \omega_0^2}{\tilde{\omega}_j^2 - \tilde{\omega}_j'^2} \sqrt{\frac{\omega_{\text{pl}}^4}{\tilde{\omega}_j^4} + \frac{\nu_{\text{pn}}^2 \omega_{\text{pl}}^2}{(\tilde{\omega}_j^2 - \omega_0^2)^2}},$$

$j' \neq j$ , and  $V = S\ell$ . In the absence of phonon-photon coupling ( $\nu_{\text{pn}} = 0$ ), the two modes  $j = 1, 2$  reduce to the bare phonon and plasmon. A similar situation occurs for  $\nu_{\text{pn}} \neq 0$ , in the case of large plasmon-phonon detunings. Both in the high  $\omega_{\text{pl}} \gg \omega_0$  and low  $\omega_{\text{pl}} \ll \omega_0$  electron density regimes, the hybrid modes reduce to the bare plasmon and phonon excitations, and the plasmon contribution prevails in the polarization field Eq. (3). This simply results in the formation of SPPs in addition to the bare phonons, with renormalized frequency  $\tilde{\omega}_0$  in the case  $\omega_{\text{pl}} \ll \omega_0$  (Fig. 1). In the following, we focus on the most interesting case occurring close to the resonance  $\omega_{\text{pl}} \sim \omega_0$ , where plasmon-phonon hybridization occurs.

*ii) Coupling to photons:* The 3D wave vector can be split into an in-plane and a transverse component in each media as  $\mathbf{Q} = q\mathbf{u}_{\parallel} + i\gamma_n \mathbf{u}_z$ , where  $n = \text{d, cr}$  refers to the dielectric medium and the crystal, respectively. For a given interface lying at the height  $z_0$ , the electromagnetic field associated to surface waves

decays exponentially on both sides as  $e^{\pm\gamma_n(z-z_0)}$  with the (real) penetration depth  $\gamma_n$ . The displacement and magnetic fields can be written as superpositions of the fields generated by each interfaces  $m = 1, 2$ , namely  $\mathbf{D}(\mathbf{R}) = \sum_{\mathbf{q},m} \sqrt{\frac{4\epsilon_0\hbar c}{S}} e^{i\mathbf{q}\cdot\mathbf{r}} \mathbf{u}_{\mathbf{q}m}(z) D_{\mathbf{q}m}$  and  $\mathbf{H}(\mathbf{R}) = \sum_{\mathbf{q},m} w_q \sqrt{\frac{4\epsilon_0\hbar c}{S}} e^{i\mathbf{q}\cdot\mathbf{r}} \mathbf{v}_{\mathbf{q}m}(z) H_{\mathbf{q}m}$ , with  $w_q$  the frequency of the surface waves (still undetermined). The mode profile functions  $\mathbf{u}_{\mathbf{q}m}(z)$  and  $\mathbf{v}_{\mathbf{q}m}(z)$  depending on  $\gamma_n$  are provided in [91]. Using these expressions, the photon Hamiltonian takes the form:

$$H_{\text{pt}} = \hbar c \sum_{\mathbf{q},m,m'} \left( \mathcal{A}_q^{mm'} D_{\mathbf{q}m} D_{-\mathbf{q}m'} + \mathcal{B}_q^{mm'} H_{\mathbf{q}m} H_{-\mathbf{q}m'} \right),$$

where the overlap matrix elements  $\mathcal{A}_q^{mm'}$  and  $\mathcal{B}_q^{mm'}$  depend on the parameters  $\gamma_{\text{cr}}$  and  $\gamma_{\text{d}}$  [91]. The next step corresponds to finding the electromagnetic field eigenmodes, which consist of a symmetric and an antisymmetric mode [96], such that the photon Hamiltonian can be put in the diagonal form:

$$H_{\text{pt}} = \hbar c \sum_{\mathbf{q},\sigma=\pm} (\alpha_{q\sigma} D_{\mathbf{q}\sigma} D_{-\mathbf{q}\sigma} + \beta_{q\sigma} H_{\mathbf{q}\sigma} H_{-\mathbf{q}\sigma}),$$

with  $\alpha_{q\pm} = \mathcal{A}_q^{11} \pm \mathcal{A}_q^{12}$ ,  $\beta_{q\pm} = \mathcal{B}_q^{11} \pm \mathcal{B}_q^{12}$ ,  $D_{\mathbf{q}\pm} = (D_{\mathbf{q}2} \pm D_{\mathbf{q}1})/\sqrt{2}$  and a similar expression for  $H_{\mathbf{q}\pm}$ . The new field operators  $D_{\mathbf{q}\sigma}$  and  $H_{\mathbf{q}\sigma}$  satisfy the commutation relations  $[D_{\mathbf{q}\sigma}, H_{\mathbf{q}'\sigma'}^\dagger] = -iC_{q\sigma} \delta_{\mathbf{q},\mathbf{q}'} \delta_{\sigma,\sigma'}$ , together with the properties  $D_{\mathbf{q}\sigma}^\dagger = D_{-\mathbf{q}\sigma}$  and  $H_{\mathbf{q}\sigma}^\dagger = H_{-\mathbf{q}\sigma}$ . The constant  $C_{q\sigma}$  is determined using the Ampère's circuital law, which provides  $C_{q\sigma} = \frac{w_q}{2c\beta_{q\sigma}}$  [90, 91]. The light-matter coupling Hamiltonian  $H_{\text{mat-pt}}$  is then derived using the expression of  $\mathbf{D}(\mathbf{R})$  in the new basis together with Eq. (3). While  $\mathbf{q}$  is a good quantum number due to the in-plane translational invariance, the perpendicular wave vector of 3D plasmons  $q_z$  is not and in  $H_{\text{mat-pt}}$ , photon modes with a given  $\mathbf{q}$  interact with linear superpositions of the 3D plasmon-phonon hybrid modes exhibiting different  $q_z$ . The latter are denoted as quasi-2D ‘‘bright’’ modes, and are defined as  $\pi_{\mathbf{q}\sigma j} = \sum_{q_z,\alpha} f_{\alpha\sigma}(Q) \Pi_{\mathbf{Q}j\alpha}$ , where  $f_{\alpha\sigma}(Q)$  stem from the overlap between the displacement and the polarization fields and is determined by imposing the commutation relations  $[\pi_{\mathbf{q}\sigma j}, \pi_{\mathbf{q}'\sigma'j'}^\dagger] = \delta_{\mathbf{q},\mathbf{q}'} \delta_{\sigma,\sigma'} \delta_{j,j'}$ .

In total, the PZW Hamiltonian reads:

$$H = \hbar c \sum_{\mathbf{q},\sigma} (\alpha_{q\sigma} D_{\mathbf{q}\sigma} D_{-\mathbf{q}\sigma} + \beta_{q\sigma} H_{\mathbf{q}\sigma} H_{-\mathbf{q}\sigma}) + \sum_{\mathbf{q},\sigma,j} \hbar \tilde{\omega}_j \pi_{\mathbf{q}\sigma j}^\dagger \pi_{\mathbf{q}\sigma j} - \sum_{\mathbf{q},\sigma,j} \hbar \Omega_{q\sigma j} \left( \pi_{-\mathbf{q}\sigma j} + \pi_{\mathbf{q}\sigma j}^\dagger \right) D_{\mathbf{q}\sigma}, \quad (4)$$

with the vacuum Rabi frequency:

$$\Omega_{q\sigma j} = g_j \sqrt{\frac{c\omega_p^2}{\tilde{\omega}_j} \left[ \frac{q^2 + \gamma_{\text{cr}}^2}{\gamma_{\text{cr}}} (1 - e^{-2\gamma_{\text{cr}}\ell}) + 2\ell\sigma e^{-\gamma_{\text{cr}}\ell} (q^2 - \gamma_{\text{cr}}^2) \right]^{1/2}}.$$

*iii) Self-consistent solutions:* This Hamiltonian exhibits three positive eigenvalues in each subspace  $(\mathbf{q}, \sigma)$ , and only the lowest two [referred to as lower (LP) and upper polaritons (UP)] correspond to surface modes since located below the light cone. At this point, we have built an Hamiltonian theory providing a functional relation between the field penetration depths  $\gamma_n$  in the crystal and dielectric media ( $n = \text{cr}, \text{d}$ ) and the surface wave frequencies  $w_{q\sigma\zeta}$ , where  $\zeta = \text{LP}, \text{UP}$  refer to the lower and upper polaritons, respectively. As explained in [90], one can combine this Hamiltonian with the Helmholtz wave equation  $\epsilon_n(\omega)\omega^2/c^2 = q^2 - \gamma_n^2$  in order to determine these parameters. Specifically, we use a self-consistent algorithm which starts with a given frequency  $w_{q\sigma\text{LP}}$ , then determine  $\gamma_n$  from the Helmholtz equation with  $\epsilon_{\text{d}} = 1$  and  $\epsilon_{\text{cr}}(w_{q\sigma\text{LP}})$  given by Eq. (2), and use these  $\gamma_n$  to compute the parameters entering the Hamiltonian Eq. (4). The latter is diagonalized using the Hopfield-Bogoliubov method [91], which allows to determine the new  $w_{q\sigma\text{LP}}$ . The algorithm is applied independently for the symmetric ( $\sigma = +$ ) and antisymmetric ( $\sigma = -$ ) modes until convergence, which is ensured by the discontinuity of both light and matter fields at each interface [90].

We now use this method to study the surface polaritons in our system. As an example, we consider the case  $\omega_{\text{pl}} = 1.5\omega_0$  with different crystal thickness  $q_0\ell = 10$  [Fig. 2 a)] and  $q_0\ell = 0.01$  [Fig. 2 b)], and compute the surface polariton frequencies  $w_{q\sigma\zeta}$  (top panels), as well as their phonon ( $i = \text{pn}$ ), plasmon ( $i = \text{pl}$ ), and photon ( $i = \text{pt}$ ) admixtures  $W_{i,q\sigma}^{\text{LP}}$  for  $\nu_{\text{pn}} = 0$  and  $\nu_{\text{pn}} = 0.5\omega_0$  (bottom panels). Precise definitions of these quantities are provided in [91], and  $\ell$  and  $q$  are both normalized to  $q_0 = \omega_0/c$ . Considering typical mid-infrared phonons with  $\hbar\omega_0 \sim 0.2\text{eV}$ , the two dimensionless parameters  $q_0\ell = 10$  and  $q_0\ell = 0.01$  correspond to  $\ell = 10\mu\text{m}$  (first case) and  $\ell \sim 10\text{nm}$  (second case), respectively.

In the first case [Fig. 2 a)], the two surface modes at each interface have negligible overlap and the modes  $\sigma_{\pm}$  therefore coincide. For  $\nu_{\text{pn}} = 0$ , the plasmon-photon coupling is responsible for the appearance of a SPP mode (black line) with frequency  $\xi_q$ , which enters in resonance with the phonon mode at  $q \approx 2.2q_0$ . While for  $q \ll q_0$  this SPP is mainly composed of light ( $\xi_q \sim qc$ ), it features a hybrid plasmon-photon character for  $q \sim q_0$ , and becomes mostly plasmon-like as  $\xi_q$  approaches asymptotically the surface plasmon frequency  $\omega_{\text{pl}}/\sqrt{2}$ . For  $\nu_{\text{pn}} \neq 0$ , a splitting between the two polaritons branches (thick red and blue lines) is clearly visible, and the latter

consist of a mix between phonons, plasmons, and photons in the vicinity of  $q = q_0$ . In the regime  $q > q_0$ , since the mostly phonon-like LP exhibits a  $\sim 25\%$  plasmon admixture, this polariton mode can be seen as a “dressed” phonon with frequency red-shifted from  $\omega_0$ . Similarly, the “dressed” plasmon mode (UP) is blue-shifted from the surface mode frequency  $\omega_{\text{pl}}/\sqrt{2}$  due to its  $\sim 25\%$  phonon weight.

The frequencies of the antisymmetric LP (red lines) and UP (blue lines) at resonance are represented as a function of  $\nu_{\text{pn}}/\omega_0$  for  $\omega_{\text{pl}} = 1.5\omega_0$  on the inset. Here, the resonance is defined by the condition  $\xi_{q-} = \omega_0$ , which provides  $q \approx 2.2q_0$ . We observe that the polariton splitting  $w_{q\sigma\text{UP}} - w_{q\sigma\text{LP}}$  is symmetric with respect to  $w_{q\sigma\zeta} = \omega_0$  (black dashed line) for  $\nu_{\text{pn}} \ll \omega_0$ , and becomes asymmetric in the ultrastrong coupling regime[38], when  $\nu_{\text{pn}}$  becomes a non-negligible fraction of  $\omega_0$ . Furthermore, the splitting is found to decrease rapidly as the electronic plasma frequency  $\omega_{\text{pl}}$  is increased.

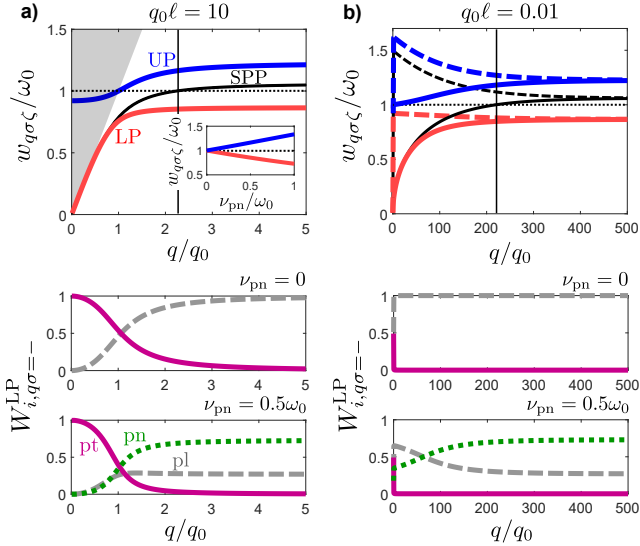


FIG. 2. Normalized frequency dispersion  $w_{q\sigma\zeta}/\omega_0$  and mode admixtures of the surface polaritons as a function of  $q/q_0$  for  $\omega_{\text{pl}} = 1.5\omega_0$ . **a)**  $q_0\ell = 10$ . **b)**  $q_0\ell = 0.01$ . Top panel: The SPPs obtained for  $\nu_{\text{pn}} = 0$  are depicted as black lines, while the surface lower and upper polaritons obtained for  $\nu_{\text{pn}} = 0.5\omega_0$  are represented as thick red and blue lines, respectively. Resonance between SPPs and phonons (horizontal dotted line) is indicated by a thin vertical line. The antisymmetric ( $\sigma = -$ ) and symmetric ( $\sigma = +$ ) modes correspond to the solid and dashed lines, and the light cone with boundary  $\omega = qc$  is represented a grey shaded region. Inset: Frequency  $w_{q\sigma\zeta}/\omega_0$  of the lower (red line) and upper (blue line) surface polaritons versus  $\nu_{\text{pn}}/\omega_0$  for  $q_0\ell = 10$  and  $\omega_{\text{pl}} = 1.5\omega_0$ . The phonon frequency is depicted as a black dotted line. Bottom panels: Plasmon (grey dashed lines), photon (magenta solid lines), and phonon (green dotted lines) admixtures of the antisymmetric lower polariton  $W_{i,q\sigma}^{\text{LP}}$  ( $i = \text{pl}, \text{pt}, \text{pn}$ ) as a function of  $q/q_0$  for  $\omega_{\text{pl}} = 1.5\omega_0$ . The top and bottom sub-panels correspond to  $\nu_{\text{pn}} = 0$  and  $\nu_{\text{pn}} = 0.5\omega_0$ , respectively.

In the second case  $q_0\ell = 0.01$  [Fig. 2 b)], the crystal is thinner than the penetration depth  $\gamma_{\text{cr}}$  of the surface waves at the two interfaces, and the latter overlap. This results in two independent sets of modes  $\sigma = \pm$  with different frequencies. For  $\nu_{\text{pn}} = 0$ , the symmetric and antisymmetric SPPs with frequency  $\xi_{q\sigma=\pm}$  are represented as black dashed and solid lines, respectively. The resonance between the symmetric SPP and the phonon mode occurs at  $q \sim q_0$ , in the regime where the symmetric SPP is mostly photon-like with  $\xi_{q\sigma=+} \sim qc$ . Interestingly, the resonance between the antisymmetric SPP and the phonon mode is now shifted to a large wave vector  $q \approx 220q_0$ , where the antisymmetric SPP exhibits a pure plasmonic character. For  $q/q_0 \rightarrow \infty$ , the two SPPs  $\sigma = \pm$  converge to the surface plasmon frequency  $\omega_{\text{pl}}/\sqrt{2}$ . For  $\nu_{\text{pn}} \neq 0$ , the antisymmetric LP (thick red solid line) and UP (thick blue solid line) are split in the vicinity of the resonance, while the symmetric polaritons (thick colored dashed lines) do not feature any anticrossing behavior  $\forall q$ . Similarly as in **a)**, the LPs  $\sigma = \pm$  can be seen as dressed phonon modes with frequencies red-shifted from  $\omega_0$  for large  $q$  due to their plasmon admixtures.

The ability to tune the energy and wave vector of the dressed phonon by respectively tuning the electronic plasma frequency and crystal thickness opens up interesting perspectives to modify the electron-phonon scattering leading to superconductivity in certain materials [97–103]. For instance, bilayer graphene with  $\ell \sim 0.7\text{nm}$  [104] exhibits an infrared-active phonon mode at  $\hbar\omega_0 = 0.2\text{eV}$  [83], and features superconductivity at low carrier densities  $\approx 2 \times 10^{12}\text{cm}^{-2}$  when the two sheets of graphene are twisted relative to each other by a small angle [103]. In this regime, we find that  $\omega_{\text{pl}} \approx \omega_0$ ,  $q_0\ell \approx 7 \times 10^{-4}$ , and the large phonon-photon coupling strengths  $\nu_{\text{pn}} \approx 0.25\omega_0$  [83] allow to reach the ultrastrong coupling regime. The typical momentum exchanged by two electrons during a scattering event induced by the electron-phonon interaction corresponds to the Fermi wave vector  $K_{\text{F}} \approx 1.6 \times 10^3 q_0$ . Despite the absence of resonance between the phonon mode and the antisymmetric SPP since  $\omega_0 > \omega_{\text{pl}}/\sqrt{2}$  in this case, we find that the antisymmetric LP for  $q \sim K_{\text{F}}$  is composed of half a phonon and half a plasmon, and occurs at low energy  $w_{q=K_{\text{F}}\sigma=-\text{LP}} \approx 0.5\omega_0$ . It is an interesting prospect to investigate whether this dressed phonon mode can affect superconductivity in bilayer graphene or other materials.

In summary, we have carried out the first quantum theory of lossless plasmon-phonon polaritons valid for arbitrary large coupling strengths, and discussed the different regimes of interest obtained by tuning the crystal thickness and the phonon-photon coupling strength. In particular, we have found that in the regime where both the electronic and ionic plasma frequencies become comparable to the phonon frequency, a dressed low-energy phonon mode with finite plasmon weight arises. For quasi-2D crystals with  $q_0\ell \ll 1$ , the in-plane wave vec-

tor of this dressed phonon can reach very large values  $\sim K_F$ , which could affect superconductivity in certain molecular crystals [97–103]. While our model specifically addresses the case of metallic crystals with rather large ionic charges supporting far/mid-infrared phonons [83–88], it can be directly generalized to describe other type of excitations such as excitons, and extended to various geometries. Further useful extensions include the case of 2D materials in the presence of disorder and dissipation.

*Acknowledgements:* We gratefully acknowledge discussions with M. Antezza, T. Chervy, V. Galitski, Y. Laplace, Stefan Schütz, A. Thomas, and Y. Todorov. This work is partially supported by the ANR - “ERANET QuantERA” - Projet “RouTe” and Labex NIE.

- 
- [1] H. Raether, *Surface plasmons on smooth and rough surfaces and on gratings* (Springer-Verlag, Berlin, Heidelberg, 1988).
- [2] W. L. Barnes, A. Dereux, and T. W. Ebbesen, *Nature* **424**, 824 (2003).
- [3] C. Genet and T. W. Ebbesen, *Nature* **445**, 39 (2007).
- [4] A. V. Akimov, A. Mukherjee, C. L. Yu, D. E. Chang, A. S. Zibrov, P. R. Hemmer, H. Park, and M. D. Lukin, *Nature* **450**, 402 (2007).
- [5] A. N. Grigorenko, M. Polini, and K. S. Novoselov, *Nature Photonics* **6**, 749 (2012).
- [6] M. Kauranen and A. V. Zayats, *Nature Photonics* **6**, 737 (2012).
- [7] N. P. de Leon, B. J. Shields, C. L. Yu, D. E. Englund, A. V. Akimov, M. D. Lukin, and H. Park, *Phys. Rev. Lett.* **108**, 226803 (2012).
- [8] V. Agranovich and A. Malshukov, *Optics Communications* **11**, 169 (1974).
- [9] V. Yakovlev, V. Nazin, and G. Zhizhin, *Optics Communications* **15**, 293 (1975).
- [10] M. R. Philpott and P. G. Sherman, *Phys. Rev. B* **12**, 5381 (1975).
- [11] I. Pockrand and J. D. Swalen, *J. Opt. Soc. Am.* **68**, 1147 (1978).
- [12] I. Pockrand, A. Brillante, and D. Möbius, *The Journal of Chemical Physics* **77**, 6289 (1982).
- [13] J. Bellessa, C. Bonnand, J. C. Plenet, and J. Mugnier, *Phys. Rev. Lett.* **93**, 036404 (2004).
- [14] J. Dintinger, S. Klein, F. Bustos, W. L. Barnes, and T. W. Ebbesen, *Phys. Rev. B* **71**, 035424 (2005).
- [15] P. Vasa, R. Pomraenke, S. Schwieger, Y. I. Mazur, V. Kunets, P. Srinivasan, E. Johnson, J. E. Kihm, D. S. Kim, E. Runge, G. Salamo, and C. Lienau, *Phys. Rev. Lett.* **101**, 116801 (2008).
- [16] D. E. Gómez, K. C. Vernon, P. Mulvaney, and T. J. Davis, *Nano Letters* **10**, 274 (2010).
- [17] P. Vasa, R. Pomraenke, G. Cirmi, E. De Re, W. Wang, S. Schwieger, D. Leipold, E. Runge, G. Cerullo, and C. Lienau, *ACS Nano* **4**, 7559 (2010).
- [18] A. Berrier, R. Cools, C. Arnold, P. Offermans, M. Crego-Calama, S. H. Brongersma, and J. Gómez-Rivas, *ACS Nano* **5**, 6226 (2011).
- [19] P. Vasa, W. Wang, R. Pomraenke, M. Lammers, M. Maiuri, C. Manzoni, G. Cerullo, and C. Lienau, *Nature Photonics* **7**, 128 (2013).
- [20] A. González-Tudela, P. A. Huidobro, L. Martín-Moreno, C. Tejedor, and F. J. García-Vidal, *Phys. Rev. Lett.* **110**, 126801 (2013).
- [21] T. Hümmer, F. J. García-Vidal, L. Martín-Moreno, and D. Zueco, *Phys. Rev. B* **87**, 115419 (2013).
- [22] E. Eizner and T. Ellenbogen, *Applied Physics Letters* **104**, 223301 (2014).
- [23] E. Orgiu, J. George, J. Hutchison, E. Devaux, J. F. Dayen, B. Doudin, F. F. Stellacci, C. Genet, J. Schachenmayer, C. Genes, G. Pupillo, P. Samori, and T. W. Ebbesen, *Nature Materials* **14**, 1123 (2015).
- [24] H. Memmi, O. Benson, S. Sadofev, and S. Kalusniak, *Phys. Rev. Lett.* **118**, 126802 (2017).
- [25] Y. Zhang, Q.-S. Meng, L. Zhang, Y. Luo, Y.-J. Yu, B. Yang, Y. Zhang, R. Esteban, J. Aizpurua, Y. Luo, J.-L. Yang, Z.-C. Dong, and J. G. Hou, *Nature Communications* **8**, 15225 (2017).
- [26] T. Chervy, S. Azzini, E. Lorchat, S. Wang, Y. Gorodetski, J. A. Hutchison, S. Berciaud, T. W. Ebbesen, and C. Genet, *ACS Photonics* **5**, 1281 (2018).
- [27] G. D. Scholes and G. Rumbles, *Nature Materials* **5**, 683 (2006).
- [28] J. A. Hutchison, T. Schwartz, C. Genet, E. Devaux, and T. W. Ebbesen, *Angew. Chem.* **51**, 1592 (2012).
- [29] A. Shalabney, J. George, J. A. Hutchison, G. Pupillo, C. Genet, and T. W. Ebbesen, *Nature Communications* **6**, 5981 (2015).
- [30] J. George, A. Shalabney, J. A. Hutchison, C. Genet, and T. W. Ebbesen, *The Journal of Physical Chemistry Letters* **6**, 1027 (2015).
- [31] R. M. A. Vergauwe, J. George, T. Chervy, J. A. Hutchison, A. Shalabney, V. Y. Torbeev, and T. W. Ebbesen, *J. Phys. Chem. Lett.* **7**, 4159 (2016).
- [32] A. D. Dunkelberger, B. T. Spann, K. P. Fears, B. S. Simpkins, and J. C. Owrutsky, *Nature Communications* **7**, 13504 (2016).
- [33] F. Herrera and F. C. Spano, *Phys. Rev. Lett.* **116**, 238301 (2016).
- [34] A. Thomas, J. George, A. Shalabney, M. Dryzhakov, S. J. Varma, J. Moran, T. Chervy, X. Zhong, E. Devaux, C. Genet, J. A. Hutchison, and T. W. Ebbesen, *Angew. Chem.* **55**, 11462 (2016).
- [35] J. Galego, F. J. Garcia-Vidal, and J. Feist, *Nature Communications* **7**, 13841 (2016).
- [36] W. Ahn, I. Vurgaftman, A. D. Dunkelberger, J. C. Owrutsky, and B. S. Simpkins, *ACS Photonics* **5**, 158 (2018).
- [37] T. Chervy, A. Thomas, E. Akiki, R. M. A. Vergauwe, A. Shalabney, J. George, E. Devaux, J. A. Hutchison, C. Genet, and T. W. Ebbesen, *ACS Photonics* **5**, 217 (2018).
- [38] C. Ciuti, G. Bastard, and I. Carusotto, *Phys. Rev. B* **72**, 115303 (2005).
- [39] P. Forn-Díaz, L. Lamata, E. Rico, J. Kono, and E. Solano, ArXiv e-prints (2018), [arXiv:1804.09275](https://arxiv.org/abs/1804.09275) [quant-ph].
- [40] A. F. Kockum, A. Miranowicz, S. De Liberato, S. Savasta, and F. Nori, ArXiv e-prints (2018), [arXiv:1807.11636](https://arxiv.org/abs/1807.11636) [cond-mat.mes-hall].
- [41] A. A. Anappara, S. De Liberato, A. Tredicucci, C. Ciuti, G. Biasiol, L. Sorba, and F. Beltram, *Phys. Rev. B* **79**, 201303 (2009).

- [42] G. Gunter, A. A. Anappara, J. Hees, A. Sell, G. Biasiol, L. Sorba, S. De Liberato, C. Ciuti, A. Tredicucci, A. Leitenstorfer, and R. Huber, *Nature* **458**, 178 (2009).
- [43] Y. Todorov, A. M. Andrews, R. Colombelli, S. De Liberato, C. Ciuti, P. Klang, G. Strasser, and C. Sirtori, *Phys. Rev. Lett.* **105**, 196402 (2010).
- [44] V. M. Muravev, I. V. Andreev, I. V. Kukushkin, S. Schmult, and W. Dietsche, *Phys. Rev. B* **83**, 075309 (2011).
- [45] T. Schwartz, J. A. Hutchison, C. Genet, and T. W. Ebbesen, *Phys. Rev. Lett.* **106**, 196405 (2011).
- [46] M. Geiser, F. Castellano, G. Scalari, M. Beck, L. Nevou, and J. Faist, *Phys. Rev. Lett.* **108**, 106402 (2012).
- [47] G. Scalari, C. Maissen, D. Turcinkova, D. Hagenmüller, S. De Liberato, C. Ciuti, C. Reichl, D. Schuh, W. Wegscheider, M. Beck, and J. Faist, *Science* **335**, 1323 (2012).
- [48] J. A. Hutchison, T. Schwartz, C. Genet, E. Devaux, and T. W. Ebbesen, *Angewandte Chemie International Edition* **51**, 1592 (2012).
- [49] S. Balci, *Opt. Lett.* **38**, 4498 (2013).
- [50] A. Cacciola, O. Di Stefano, R. Stassi, R. Saija, and S. Savasta, *ACS Nano* **8**, 11483 (2014).
- [51] M. Goryachev, W. G. Farr, D. L. Creedon, Y. Fan, M. Kostylev, and M. E. Tobar, *Phys. Rev. Applied* **2**, 054002 (2014).
- [52] Q. Zhang, M. Lou, X. Li, J. L. Reno, W. Pan, J. D. Watson, M. J. Manfra, and J. Kono, *Nature Physics* **12**, 1005 (2016).
- [53] J. George, T. Chervy, A. Shalabney, E. Devaux, H. Hiura, C. Genet, and T. W. Ebbesen, *Phys. Rev. Lett.* **117**, 153601 (2016).
- [54] F. Todisco, M. De Giorgi, M. Esposito, L. De Marco, A. Zizzari, M. Bianco, L. Dominici, D. Ballarini, V. Arima, G. Gigli, and D. Sanvitto, *ACS Photonics* **5**, 143 (2018).
- [55] A. Delga, J. Feist, J. Bravo-Abad, and F. J. Garcia-Vidal, *Journal of Optics* **16**, 114018 (2014).
- [56] A. I. Alekseev and Y. P. Nikitin, *Soviet Physics JETP* **23**, 114 (1966).
- [57] J. M. Elson and R. H. Ritchie, *Phys. Rev. B* **4**, 4129 (1971).
- [58] M. Hillery and L. D. Mlodinow, *Phys. Rev. A* **30**, 1860 (1984).
- [59] Y. Oi Nakamura, *Progress of Theoretical Physics* **74**, 1191 (1985).
- [60] T. A. B. Kennedy and E. M. Wright, *Phys. Rev. A* **38**, 212 (1988).
- [61] P. D. Drummond, *Phys. Rev. A* **42**, 6845 (1990).
- [62] B. Huttner, J. J. Baumberg, and S. M. Barnett, *EPL* **16**, 177 (1991).
- [63] P. Milonni, *Journal of Modern Optics* **42**, 1991 (1995).
- [64] T. Gruner and D.-G. Welsch, *Phys. Rev. A* **53**, 1818 (1996).
- [65] H. T. Dung, L. Knöll, and D.-G. Welsch, *Phys. Rev. A* **57**, 3931 (1998).
- [66] R. Matloob, *Phys. Rev. A* **60**, 50 (1999).
- [67] O. Di Stefano, S. Savasta, and R. Girlanda, *Phys. Rev. A* **61**, 023803 (2000).
- [68] H. T. Dung, S. Y. Buhmann, L. Knöll, D.-G. Welsch, S. Scheel, and J. Kästel, *Phys. Rev. A* **68**, 043816 (2003).
- [69] J. C. Garrison and R. Y. Chiao, *Phys. Rev. A* **70**, 053826 (2004).
- [70] S. Stallinga, *Phys. Rev. E* **73**, 026606 (2006).
- [71] N. A. R. Bhat and J. E. Sipe, *Phys. Rev. A* **73**, 063808 (2006).
- [72] M. S. Tame, C. Lee, J. Lee, D. Ballester, M. Paternostro, A. V. Zayats, and M. S. Kim, *Phys. Rev. Lett.* **101**, 190504 (2008).
- [73] A. Archambault, T. V. Teperik, F. Marquier, and J.-J. Greffet, *Phys. Rev. B* **79**, 195414 (2009).
- [74] A. Archambault, F. Marquier, J.-J. Greffet, and C. Arnold, *Phys. Rev. B* **82**, 035411 (2010).
- [75] S. A. R. Horsley and T. G. Philbin, *New Journal of Physics* **16**, 013030 (2014).
- [76] J. Askne, *Journal of Physics A: General Physics* **5**, 1578 (1972).
- [77] M. Artoni and J. L. Birman, *Phys. Rev. B* **44**, 3736 (1991).
- [78] M. Babiker, N. C. Constantinou, and B. K. Ridley, *Phys. Rev. B* **48**, 2236 (1993).
- [79] C. R. Gubbin, S. A. Maier, and S. De Liberato, *Phys. Rev. B* **94**, 205301 (2016).
- [80] C. R. Gubbin and S. De Liberato, *ACS Photonics* **5**, 284 (2018).
- [81] G. D. Mahan, *Many-Particle Physics*, 2nd ed. (Plenum, New York, N.Y., 1993).
- [82] D. Mirlin, *Surface Polaritons*, edited by V. Agranovitch and D. Mills (Elsevier, 1982).
- [83] A. B. Kuzmenko, L. Benfatto, E. Cappelluti, I. Crassee, D. van der Marel, P. Blake, K. S. Novoselov, and A. K. Geim, *Phys. Rev. Lett.* **103**, 116804 (2009).
- [84] M. J. Rice and H.-Y. Choi, *Phys. Rev. B* **45**, 10173 (1992).
- [85] K.-J. Fu, W. L. Karney, O. L. Chapman, S.-M. Huang, R. B. Kaner, F. Diederich, K. Holczer, and R. L. Whetten, *Phys. Rev. B* **46**, 1937 (1992).
- [86] M. J. Rice, N. O. Lipari, and S. Strässler, *Phys. Rev. Lett.* **39**, 1359 (1977).
- [87] D. B. Tanner, C. S. Jacobsen, A. A. Bright, and A. J. Heeger, *Phys. Rev. B* **16**, 3283 (1977).
- [88] M. S. Khatkale and J. P. Devlin, *The Journal of Chemical Physics* **70**, 1851 (1979).
- [89] A. Damascelli, K. Schulte, D. van der Marel, and A. A. Menovsky, *Phys. Rev. B* **55**, R4863 (1997).
- [90] Y. Todorov, *Phys. Rev. B* **89**, 075115 (2014).
- [91] D. Hagenmüller, J. Schachenmayer, C. Genet, T. Ebbesen, and G. Pupillo, Supplemental Material for “Intrinsic surface plasmon-phonon polaritons: A non-perturbative quantum theory” (2018).
- [92] M. Babiker and R. Loudon, *Proc. R. Soc. Lond. A* **385**, 439 (1983).
- [93] C. Cohen-Tannoudji, J. Dupont-Roc, and G. Grynberg, *Photons and Atoms: Introduction to Quantum Electrodynamics*, 2nd ed. (Wiley-VCH, 1997).
- [94] Our method can be easily generalized when phonons are replaced by excitons, by considering the appropriate polarization field.
- [95] D. Bohm and D. Pines, *Phys. Rev.* **92**, 609 (1953).
- [96] S. A. Maier, *Plasmonics: Fundamentals and Applications* (Springer US, 2007).
- [97] K. Tanigaki, T. W. Ebbesen, S. Saito, J. Mizuki, J. S. Tsai, Y. Kubo, and S. Kuroshima, *Nature* **352**, 222 (1991).
- [98] O. Gunnarsson, *Rev. Mod. Phys.* **69**, 575 (1997).
- [99] D. Jérôme, *Chemical Reviews* **104**, 5565 (2004).
- [100] K. Ueno, S. Nakamura, H. Shimotani, A. Ohtomo, N. Kimura, T. Nojima, H. Aoki, Y. Iwasa, and

- M. Kawasaki, *Nature Materials* **7**, 855 (2008).
- [101] W. Qing-Yan, L. Zhi, Z. Wen-Hao, Z. Zuo-Cheng, Z. Jin-Song, L. Wei, D. Hao, O. Yun-Bo, D. Peng, C. Kai, W. Jing, S. Can-Li, H. Ke, J. Jin-Feng, J. Shuai-Hua, W. Ya-Yu, W. Li-Li, C. Xi, M. Xu-Cun, and X. Qi-Kun, *Chinese Physics Letters* **29**, 037402 (2012).
- [102] W. Shi, J. Ye, Y. Zhang, R. Suzuki, M. Yoshida, J. Miyazaki, N. Inoue, Y. Saito, and Y. Iwasa, *Scientific Reports* **5**, 12534 (2015).
- [103] Y. Cao, V. Fatemi, S. Fang, K. Watanabe, T. Taniguchi, E. Kaxiras, and P. Jarillo-Herrero, *Nature* **556**, 43 (2018).
- [104] I. Razado-Colambo, J. Avila, D. Vignaud, S. Godey, X. Wallart, D. P. Woodruff, and M. C. Asensio, *Scientific Reports* **8**, 10190 (2018).
- [105] J. J. Hopfield, *Phys. Rev.* **112**, 1555 (1958).
- [106] J. Lindhard, *Kgl. Danske Vidensk. Selsk. Mater.-fys. Medd.* **28**, 1 (1954).

## SUPPLEMENTAL MATERIAL

In this supplemental material, we provide details of the calculations sketched in the main text. The first section is dedicated to the derivation and diagonalization of the matter Hamiltonian leading to hybrid plasmon-phonon modes, and the second section to the light-matter coupling Hamiltonian involving photonic degrees of freedom. We explain the self-consistent Hamiltonian method in detail and define the plasmon, phonon, and photon admixtures of the surface polaritons. Further details concerning the theoretical foundations of the model can be found in Ref. [90]. In the last section, we study an elementary plasmonic structure composed of a single metal-dielectric interface, where phonons in the dielectric region strongly interact with SPPs. We use an effective model similar to that of Refs. [20 and 21], which is based on the SPP quantization scheme detailed in Refs. [57, 59, 72–74], and show that unphysical behaviors appear in the ultrastrong coupling regime.

### Matter Hamiltonian

The matter Hamiltonian involves both electronic and phononic degrees of freedom through the total polarization field  $\mathbf{P} = \mathbf{P}_{\text{pl}} + \mathbf{P}_{\text{pn}}$ , where

$$\mathbf{P}_{\text{pl}}(\mathbf{R}) = \frac{1}{V} \sum_{\mathbf{K}, \mathbf{Q}} \boldsymbol{\xi}_{\mathbf{K}\mathbf{Q}} \left( P_{-\mathbf{K}-\mathbf{Q}} + P_{\mathbf{K}\mathbf{Q}}^\dagger \right) e^{-i\mathbf{Q}\cdot\mathbf{R}} \quad (5)$$

denotes the plasmon polarization field and  $\mathbf{P}_{\text{pn}}$  the phonon polarization. In the case of a 3D free electron gas, the electron-hole excitation operator  $P_{\mathbf{K}\mathbf{Q}}^\dagger = c_{\mathbf{K}+\mathbf{Q}}^\dagger c_{\mathbf{K}}$  involves the fermionic operators  $c_{\mathbf{K}}$  and  $c_{\mathbf{K}}^\dagger$ , which annihilates and creates an electron with 3D wave vector  $\mathbf{K}$ , respectively. For long-wavelength excitations with  $Q \ll K_F$ , the Hilbert space is restricted to the RPA subspace spanned by the states  $\{|F\rangle, P_{\mathbf{K}\mathbf{Q}}^\dagger |F\rangle\}$ , where  $|F\rangle = \prod_{K < K_F} c_{\mathbf{K}}^\dagger |0\rangle$  is the electron ground state (Fermi sea of the free electron gas),  $K = |\mathbf{K}|$  the wave vector modulus,  $|0\rangle$  the vacuum state, and  $K_F$  the Fermi wave vector. In this case, it can be shown [90] that  $P_{\mathbf{K}\mathbf{Q}}^\dagger$  and its hermitian conjugate are bosonic operators satisfying the commutation relation  $[P_{\mathbf{K}\mathbf{Q}}, P_{\mathbf{K}'\mathbf{Q}'}^\dagger] = \delta_{\mathbf{K}, \mathbf{K}'} \delta_{\mathbf{Q}, \mathbf{Q}'}$ . The electronic dipole moment reads  $\boldsymbol{\xi}_{\mathbf{K}\mathbf{Q}} = -ien_{\mathbf{K}}(1 - n_{\mathbf{K}+\mathbf{Q}}) \frac{2\mathbf{K}+\mathbf{Q}}{(2\mathbf{K}+\mathbf{Q})\cdot\mathbf{Q}}$ , where  $n_{\mathbf{K}}$  denotes the Fermi occupation number at zero temperature, namely  $n_{\mathbf{K}} = 1$  for  $K < K_F$  and  $n_{\mathbf{K}} = 0$  for  $K > K_F$ . The electron charge and mass are denoted as  $e$  and  $m$ , respectively.

Denoting the lattice site positions as  $\mathbf{R}_i$ , where  $i \in [1, n]$  with  $n$  the number of unit cell in the crystal, the phonon polarization field can be written as:

$$\mathbf{P}_{\text{pn}}(\mathbf{R}) = \sqrt{\frac{Z^2 N \hbar}{2M\omega_0}} \sum_{\alpha, i} \delta(\mathbf{R} - \mathbf{R}_i) \left( B_{i\alpha} + B_{i\alpha}^\dagger \right) \mathbf{u}_\alpha. \quad (6)$$

Here,  $\mathbf{u}_\alpha$  with  $\alpha = z, //$  denotes the polarization vector of each phonon mode with the same frequency  $\omega_0$ ,  $N$  the number of vibrating ions with effective mass  $M$  and charge  $Z$  per unit cell, and  $B_{i\alpha}$  and  $B_{i\alpha}^\dagger$  respectively annihilates and creates a phonon polarized in the direction  $\alpha$  at the lattice position  $i$ . These operators satisfy the bosonic commutation relation  $[B_{i\alpha}, B_{i'\alpha'}^\dagger] = \delta_{\alpha, \alpha'} \delta_{i, i'}$ . Writing the phonon operators in the Fourier basis:  $B_{i\alpha} = \frac{1}{\sqrt{n}} \sum_{\mathbf{Q}} B_{\mathbf{Q}\alpha} e^{-i\mathbf{Q}\cdot\mathbf{R}_i}$ , the

phonon polarization Eq. (6) takes the form:

$$\mathbf{P}_{\text{pn}}(\mathbf{R}) = \sqrt{\frac{Z^2 N \hbar}{2M\omega_0 V a^3}} \sum_{\mathbf{Q}, \alpha} \left( B_{-\mathbf{Q}\alpha} + B_{\mathbf{Q}\alpha}^\dagger \right) \mathbf{u}_\alpha e^{-i\mathbf{Q}\cdot\mathbf{R}}, \quad (7)$$

with  $a^3$  the volume of a unit cell. The matter Hamiltonian can be decomposed as  $H_{\text{mat}} = H_{\text{pl}} + H_{\text{pn}} + H_{\text{P}^2}$ .  $H_{\text{pl}} = \sum_{\mathbf{K}, \mathbf{Q}} \hbar \Delta\omega_{\mathbf{K}, \mathbf{Q}} P_{\mathbf{K}\mathbf{Q}}^\dagger P_{\mathbf{K}\mathbf{Q}}$  is the effective Hamiltonian providing the energy of the electron-hole pairs created across the Fermi sea  $\Delta\omega_{\mathbf{K}, \mathbf{Q}} = \omega_{\mathbf{K}+\mathbf{Q}} - \omega_{\mathbf{K}}$ , with  $\omega_{\mathbf{K}} = \hbar K^2/2m$ . The free phonon Hamiltonian reads  $H_{\text{pn}} = \sum_{\mathbf{Q}, \alpha} \hbar\omega_0 B_{\mathbf{Q}\alpha}^\dagger B_{\mathbf{Q}\alpha}$ , and the interaction term  $H_{\text{P}^2}$  is proportional to the square polarization field:

$$H_{\text{P}^2} = \frac{1}{2\epsilon_0} \int d\mathbf{R} \mathbf{P}^2(\mathbf{R}). \quad (8)$$

This term thus contains the contributions of both plasmons and phonons  $\propto \mathbf{P}_{\text{pl}}^2$  and  $\propto \mathbf{P}_{\text{pn}}^2$ , respectively, as well as a direct interaction term  $\propto \mathbf{P}_{\text{pl}} \cdot \mathbf{P}_{\text{pn}}$  between electronic and phononic excitations. Replacing Eqs. (5) and (7) into Eq. (8) and performing the spatial integration, the matter Hamiltonian is derived as:

$$\begin{aligned} H_{\text{mat}} = & \sum_{\mathbf{K}, \mathbf{Q}} \hbar \Delta\omega_{\mathbf{K}, \mathbf{Q}} P_{\mathbf{K}\mathbf{Q}}^\dagger P_{\mathbf{K}\mathbf{Q}} + \sum_{\mathbf{Q}, \alpha} \hbar\omega_0 B_{\mathbf{Q}\alpha}^\dagger B_{\mathbf{Q}\alpha} + \sum_{\mathbf{K}, \mathbf{K}', \mathbf{Q}} \hbar \Lambda_{\mathbf{K}\mathbf{K}'}^{\mathbf{Q}} \left( P_{-\mathbf{K}-\mathbf{Q}} + P_{\mathbf{K}\mathbf{Q}}^\dagger \right) \left( P_{\mathbf{K}'\mathbf{Q}} + P_{-\mathbf{K}'-\mathbf{Q}}^\dagger \right) \\ & + \sum_{\mathbf{Q}, \alpha} \frac{\hbar\nu_{\text{p}}^2}{4\omega_0} \left( B_{-\mathbf{Q}\alpha} + B_{\mathbf{Q}\alpha}^\dagger \right) \left( B_{\mathbf{Q}\alpha} + B_{-\mathbf{Q}\alpha}^\dagger \right) + \sum_{\mathbf{K}, \mathbf{Q}, \alpha} \hbar \lambda_{\mathbf{K}\mathbf{Q}}^\alpha \left( P_{-\mathbf{K}-\mathbf{Q}} + P_{\mathbf{K}\mathbf{Q}}^\dagger \right) \left( B_{\mathbf{Q}\alpha} + B_{-\mathbf{Q}\alpha}^\dagger \right), \end{aligned} \quad (9)$$

where we have introduced  $\Lambda_{\mathbf{K}\mathbf{K}'}^{\mathbf{Q}} = \frac{1}{2\epsilon_0 \hbar V} \boldsymbol{\xi}_{\mathbf{K}\mathbf{Q}} \cdot \boldsymbol{\xi}_{\mathbf{K}'\mathbf{Q}}$  and  $\lambda_{\mathbf{K}\mathbf{Q}}^\alpha = \frac{\nu_{\text{pn}}}{\sqrt{2\epsilon_0 \hbar \omega_0 V}} \boldsymbol{\xi}_{\mathbf{K}\mathbf{Q}} \cdot \mathbf{u}_\alpha$ . The Hamiltonian Eq. (9) can be diagonalized using the Hopfield-Bogoliubov method [105], by introducing collective eigenmodes on the form:

$$\Pi_{\mathbf{Q}j} = \sum_{\mathbf{K}} \left( a_{\mathbf{K}\mathbf{Q}j} P_{\mathbf{K}\mathbf{Q}} + \tilde{a}_{\mathbf{K}\mathbf{Q}j} P_{-\mathbf{K}-\mathbf{Q}}^\dagger \right) + \sum_{\alpha} \left( b_{\mathbf{Q}\alpha j} B_{\mathbf{Q}\alpha} + \tilde{b}_{\mathbf{Q}\alpha j} B_{-\mathbf{Q}\alpha}^\dagger \right). \quad (10)$$

The condition for these modes to diagonalize the Hamiltonian Eq. (9) is then  $[\Pi_{\mathbf{Q}j}, H_{\text{mat}}] = \hbar\tilde{\omega}_j \Pi_{\mathbf{Q}j}$ . Computing this commutator and introducing the vector:

$$\mathbf{Z}_{\mathbf{Q}j} = \sum_{\mathbf{K}} \frac{\boldsymbol{\xi}_{\mathbf{K}\mathbf{Q}}}{2\epsilon_0 \hbar V} (a_{\mathbf{K}\mathbf{Q}j} - \tilde{a}_{\mathbf{K}\mathbf{Q}j}) + \sum_{\alpha} \frac{\nu_{\text{pn}} \mathbf{u}_\alpha}{\sqrt{8\epsilon_0 \hbar V} \omega_0} (b_{\mathbf{K}\mathbf{Q}j} - \tilde{b}_{\mathbf{K}\mathbf{Q}j}), \quad (11)$$

we obtain the following relations for the transformation coefficients entering Eq. (10):

$$\begin{aligned} a_{\mathbf{K}\mathbf{Q}j} &= \frac{-2\boldsymbol{\xi}_{\mathbf{K}\mathbf{Q}} \cdot \mathbf{Z}_{\mathbf{Q}j}}{\tilde{\omega}_j - \Delta\omega_{\mathbf{K}, \mathbf{Q}}} & \tilde{a}_{\mathbf{K}\mathbf{Q}j} &= \frac{-2\boldsymbol{\xi}_{\mathbf{K}\mathbf{Q}} \cdot \mathbf{Z}_{\mathbf{Q}j}}{\tilde{\omega}_j + \Delta\omega_{\mathbf{K}, \mathbf{Q}}} \\ b_{\mathbf{Q}\alpha j} &= \nu_{\text{pn}} \sqrt{\frac{2\epsilon_0 \hbar V}{\omega_0}} \frac{\mathbf{u}_\alpha \cdot \mathbf{Z}_{\mathbf{Q}j}}{\tilde{\omega}_j - \omega_0} & \tilde{b}_{\mathbf{Q}\alpha j} &= \nu_{\text{pn}} \sqrt{\frac{2\epsilon_0 \hbar V}{\omega_0}} \frac{\mathbf{u}_\alpha \cdot \mathbf{Z}_{\mathbf{Q}j}}{\tilde{\omega}_j + \omega_0}. \end{aligned} \quad (12)$$

Introducing the orthogonal basis  $(\mathbf{Q}/Q, \mathbf{u}_{\mathbf{Q}1}, \mathbf{u}_{\mathbf{Q}2})$ , where  $\mathbf{u}_{\mathbf{Q}p}$  ( $p = 1, 2$ ) denote the two transverse polarization vectors,  $\mathbf{Z}_{\mathbf{Q}j}$  can be decomposed into its longitudinal and transverse components. Solving for the transverse components, one can replace  $\mathbf{Z}_{\mathbf{Q}j} = Z_{\mathbf{Q}j} \mathbf{u}_{\mathbf{Q}p}$  in Eq. (12), and Eq. (11) turns out to be equivalent to  $\epsilon_{\text{cr}}(\tilde{\omega}_j) \mathbf{Z}_{\mathbf{Q}j} = 0$ , where

$$\epsilon_{\text{cr}}(\omega) = 1 - \frac{\omega_{\text{pl}}^2}{\omega^2} - \frac{\nu_{\text{pn}}^2}{\omega^2 - \omega_0^2} \quad (13)$$

represents the transverse dielectric function of the crystal. To obtain this result, we have used the definition of the electronic plasma frequency  $\omega_{\text{pl}} = \sqrt{\frac{\rho e^2}{m\epsilon_0}}$  with  $\rho$  the electron density,  $\sum_{\alpha} \mathbf{u}_\alpha \cdot \mathbf{u}_{\mathbf{Q}, p} = 1$ , as well as the identity:

$$\frac{1}{\hbar\epsilon_0 V} \sum_{\mathbf{K}} \frac{2|\boldsymbol{\xi}_{\mathbf{K}\mathbf{Q}} \cdot \mathbf{u}_{\mathbf{Q}p}|^2 \Delta\omega_{\mathbf{K}, \mathbf{Q}}}{\omega^2 - \Delta\omega_{\mathbf{K}, \mathbf{Q}}^2} \sim \frac{\omega_{\text{pl}}^2}{\omega^2}, \quad (14)$$



in the so-called dynamical long-wavelength limit  $Q/K_F \ll 1$ ,  $\omega/\omega_F \gg Q/K_F$  ( $\omega_F = \hbar K_F^2/2m$  is the Fermi energy). Note that in this regime:

$$|\boldsymbol{\xi}_{\mathbf{K}\mathbf{Q}} \cdot \mathbf{u}_{\mathbf{Q}p}|^2 = \frac{4e^2 n_{\mathbf{K}} (1 - n_{\mathbf{K}+\mathbf{Q}}) \left[ (QK)^2 - (\mathbf{K} \cdot \mathbf{Q})^2 \right]}{Q^2 (Q^2 + 2\mathbf{K} \cdot \mathbf{Q})^2} \sim \frac{e^2 n_{\mathbf{K}} (1 - n_{\mathbf{K}+\mathbf{Q}})}{Q^2},$$

and Eq. (14) reduces to the Lindhard function which describes the longitudinal response of a free electron gas [106]. The two eigenvalues  $\tilde{\omega}_j$  can be determined by solving the equation  $\epsilon_{\text{cr}}(\tilde{\omega}_j) = 0$ , which provides the solutions given by Eq. (1) of the main text. As explained in detail in Ref. [90], the vector  $\mathbf{Z}_{\mathbf{Q}j}$  can be decomposed as  $\mathbf{Z}_{\mathbf{Q}j} = N_j R_j \mathbf{u}_{\mathbf{Q}p}$  when solving for the transverse modes, where  $R_j$  are determined by computing the residues of the inverse dielectric function:

$$\frac{1}{\epsilon_{\text{cr}}(\omega)} = 1 + \sum_{j=1,2} \frac{R_j^2}{\omega^2 - \tilde{\omega}_j^2},$$

and are derived as:

$$R_2^2 = \frac{\omega_{\text{pl}}^2 (\tilde{\omega}_2^2 - \omega_0^2) + \nu_{\text{pn}}^2 \tilde{\omega}_2^2}{\tilde{\omega}_2^2 - \tilde{\omega}_1^2} \quad R_1^2 = \frac{\omega_{\text{pl}}^2 (\tilde{\omega}_1^2 - \omega_0^2) + \nu_{\text{pn}}^2 \tilde{\omega}_1^2}{\tilde{\omega}_1^2 - \tilde{\omega}_2^2}. \quad (15)$$

The constant  $N_j$  can be found by using the normalization condition:

$$\sum_{\mathbf{K}} (|a_{\mathbf{K}\mathbf{Q}j}|^2 - |\tilde{a}_{\mathbf{K}\mathbf{Q}j}|^2) + \sum_{\alpha} (|b_{\mathbf{Q}\alpha j}|^2 - |\tilde{b}_{\mathbf{Q}\alpha j}|^2) = 1,$$

stemming from the commutation relation  $[\Pi_{\mathbf{Q}j}, \Pi_{\mathbf{Q}'j'}^\dagger] = \delta_{\mathbf{Q},\mathbf{Q}'} \delta_{j,j'}$ . Using Eq. (12) with  $\mathbf{Z}_{\mathbf{Q}j} = N_j R_j \mathbf{u}_{\mathbf{Q}p}$ , as well as the identity:

$$\frac{1}{\hbar \epsilon_0 V} \sum_{\mathbf{K}} \frac{2|\boldsymbol{\xi}_{\mathbf{K}\mathbf{Q}} \cdot \mathbf{u}_{\mathbf{Q}p}|^2 \Delta\omega_{\mathbf{K},\mathbf{Q}}}{(\omega^2 - \Delta\omega_{\mathbf{K},\mathbf{Q}}^2)^2} \sim \frac{\omega_{\text{pl}}^2}{\omega^4},$$

which can be derived similarly as Eq. (14) in the dynamical long-wavelength limit, we obtain:

$$\frac{1}{N_j^2} = 8\hbar \epsilon_0 V \tilde{\omega}_j R_j^2 \left( \frac{\omega_{\text{pl}}^2}{\tilde{\omega}_j^4} + \frac{\nu_{\text{pn}}^2}{(\tilde{\omega}_j^2 - \omega_0^2)^2} \right). \quad (16)$$

Finally, we use Eqs. (5), (7), (10), (12), the decomposition  $\mathbf{Z}_{\mathbf{Q}j} = N_j R_j \mathbf{u}_{\mathbf{Q}p}$ , as well as the identities

$$\sum_j \frac{R_j^2}{\tilde{\omega}_j^2 - \Delta\omega_{\mathbf{K},\mathbf{Q}}^2} = 1 \quad \sum_j \frac{R_j^2}{\tilde{\omega}_j^2 - \omega_0^2} = 1,$$

to write the total (transverse) polarization field as:

$$\mathbf{P}(\mathbf{R}) = \sum_{\mathbf{Q},j,p} \frac{R_j}{4N_j \tilde{\omega}_j V} \left( \Pi_{-\mathbf{Q}jp} + \Pi_{\mathbf{Q}jp}^\dagger \right) e^{-i\mathbf{Q} \cdot \mathbf{R}} \mathbf{u}_{\mathbf{Q}p}. \quad (17)$$

Since the crystal is assumed to be isotropic, one can choose the transverse polarization vectors  $\mathbf{u}_{\mathbf{Q}p}$  to coincide with  $\mathbf{u}_\alpha$  ( $\alpha = z, //$ ), and using Eqs. (15) and (16), the polarization field Eq. (17) coincides with Eq. (3) of the main text. In the new basis, the matter Hamiltonian takes the simple form:

$$H_{\text{mat}} = \sum_{\mathbf{Q},\alpha,j} \hbar \tilde{\omega}_j \Pi_{\mathbf{Q}j\alpha}^\dagger \Pi_{\mathbf{Q}j\alpha} + H_{\text{dark}},$$

where  $H_{\text{dark}}$  denotes the neglected contribution of the “dark” modes associated with the electron-hole continuum of incoherent excitations.

### Light-matter coupling Hamiltonian

In order to derive the light-matter coupling Hamiltonian  $H_{\text{mat-pt}}$ , we first need the expression of the displacement field  $\mathbf{D}(\mathbf{R})$ . The latter can be found by generalizing Todorov's approach [90] to the case of a double interface, writing  $\mathbf{D}$  as a superposition of the fields generated by each interfaces  $m = 1, 2$ , namely  $\mathbf{D}(\mathbf{R}) = \sum_{\mathbf{q}, m} \sqrt{\frac{4\epsilon_0 \hbar c}{S}} e^{i\mathbf{q}\cdot\mathbf{r}} \mathbf{u}_{\mathbf{q}m}(z) D_{\mathbf{q}m}$ , and  $\mathbf{H}(\mathbf{R}) = \sum_{\mathbf{q}, m} w_q \sqrt{\frac{4\epsilon_0 \hbar c}{S}} e^{i\mathbf{q}\cdot\mathbf{r}} \mathbf{v}_{\mathbf{q}m}(z) H_{\mathbf{q}m}$  for the magnetic field. Here,  $w_q$  denotes the frequency of the surface modes which are still undetermined at this point. Denoting by  $\mathbf{u}_\perp$  the in-plane unit vector perpendicular to both  $\mathbf{u}_z$  and  $\mathbf{u}_\parallel$ , the mode functions read:

$$\begin{aligned} \mathbf{u}_{\mathbf{q}1}(z) &= \left[ -\gamma_d \theta(-z) e^{\gamma_d z} + \gamma_{\text{cr}} \theta(z) \theta(\ell - z) e^{-\gamma_{\text{cr}} z} + \gamma_d \theta(z - \ell) e^{-\gamma_{\text{cr}} \ell} e^{-\gamma_d(z - \ell)} \right] \mathbf{u}_\parallel \\ &\quad + iq \left[ \theta(-z) e^{\gamma_d z} + \theta(z) \theta(\ell - z) e^{-\gamma_{\text{cr}} z} + \theta(z - \ell) e^{-\gamma_{\text{cr}} \ell} e^{-\gamma_d(z - \ell)} \right] \mathbf{u}_z \\ \mathbf{u}_{\mathbf{q}2}(z) &= \left[ -\gamma_d \theta(-z) e^{-\gamma_{\text{cr}} \ell} e^{\gamma_d z} - \gamma_{\text{cr}} \theta(z) \theta(\ell - z) e^{\gamma_{\text{cr}}(z - \ell)} + \gamma_d \theta(z - \ell) e^{-\gamma_d(z - \ell)} \right] \mathbf{u}_\parallel \\ &\quad + iq \left[ \theta(-z) e^{-\gamma_{\text{cr}} \ell} e^{\gamma_d z} + \theta(z) \theta(\ell - z) e^{\gamma_{\text{cr}}(z - \ell)} + \theta(z - \ell) e^{-\gamma_d(z - \ell)} \right] \mathbf{u}_z, \end{aligned}$$

and

$$\begin{aligned} \mathbf{v}_{\mathbf{q}1}(z) &= \left[ \theta(-z) e^{\gamma_d z} + \theta(z) \theta(\ell - z) e^{-\gamma_{\text{cr}} z} + \theta(z - \ell) e^{-\gamma_{\text{cr}} \ell} e^{-\gamma_d(z - \ell)} \right] \mathbf{u}_\perp \\ \mathbf{v}_{\mathbf{q}2}(z) &= \left[ \theta(-z) e^{-\gamma_{\text{cr}} \ell} e^{\gamma_d z} + \theta(z) \theta(\ell - z) e^{\gamma_{\text{cr}}(z - \ell)} + \theta(z - \ell) e^{-\gamma_d(z - \ell)} \right] \mathbf{u}_\perp. \end{aligned}$$

Replacing these expressions into  $H_{\text{pt}} = \frac{1}{2\epsilon_0} \int d\mathbf{R} \mathbf{D}^2(\mathbf{R}) + \frac{1}{2\epsilon_0 c^2} \int d\mathbf{R} \mathbf{H}^2(\mathbf{R})$  and performing the integrations, the free photon Hamiltonian is derived as:

$$H_{\text{pt}} = \hbar c \sum_{\mathbf{q}, m, m'} \left( \mathcal{A}_q^{mm'} D_{\mathbf{q}m} D_{-\mathbf{q}m'} + \mathcal{B}_q^{mm'} H_{\mathbf{q}m} H_{-\mathbf{q}m'} \right), \quad (18)$$

with the overlap matrix elements:

$$\begin{aligned} \mathcal{A}_q^{mm'} &= \frac{q^2 + \gamma_{\text{cr}}^2}{\gamma_{\text{cr}}} (1 - e^{-2\gamma_{\text{cr}} \ell}) + \frac{q^2 + \gamma_d^2}{\gamma_d} (1 + e^{-2\gamma_{\text{cr}} \ell}) \\ \mathcal{B}_q^{mm'} &= \frac{\omega_q^2}{c^2} \left( \frac{1 - e^{-2\gamma_{\text{cr}} \ell}}{\gamma_{\text{cr}}} + \frac{1 + e^{-2\gamma_{\text{cr}} \ell}}{\gamma_d} \right) \end{aligned}$$

for  $m = m'$ , and

$$\begin{aligned} \mathcal{A}_q^{mm'} &= 2e^{-2\gamma_{\text{cr}} \ell} \left[ (q^2 - \gamma_{\text{cr}}^2) \ell + \frac{q^2 + \gamma_d^2}{\gamma_d} \right] \\ \mathcal{B}_q^{mm'} &= \frac{2\omega_q^2}{c^2} e^{-2\gamma_{\text{cr}} \ell} \left( \frac{1 + \gamma_d \ell}{\gamma_d} \right) \end{aligned}$$

for  $m \neq m'$ . The Hamiltonian Eq. (18) is diagonalized by the transformation  $D_{\mathbf{q}\pm} = (D_{\mathbf{q}2} \pm D_{\mathbf{q}1}) / \sqrt{2}$ , where the new field operators  $D_{\mathbf{q}\sigma}$  and  $H_{\mathbf{q}\sigma}$  satisfy the commutation relations  $[D_{\mathbf{q}\sigma}^\dagger, D_{\mathbf{q}'\sigma'}^\dagger] = [H_{\mathbf{q}\sigma}^\dagger, H_{\mathbf{q}'\sigma'}^\dagger] = 0$ , and  $[D_{\mathbf{q}\sigma}, H_{\mathbf{q}'\sigma'}^\dagger] = -iC_{q\sigma} \delta_{\mathbf{q}, \mathbf{q}'} \delta_{\sigma, \sigma'}$ , together with the properties  $D_{\mathbf{q}\sigma}^\dagger = D_{-\mathbf{q}\sigma}$  and  $H_{\mathbf{q}\sigma}^\dagger = H_{-\mathbf{q}\sigma}$ . The constant  $C_{q\sigma}$  can be determined by using the Maxwell's equation:

$$\frac{d}{dt} \mathbf{D}(\mathbf{R}) = \frac{i}{\hbar} [H_{\text{pt}}, \mathbf{D}(\mathbf{R})] = \nabla \times \mathbf{H}(\mathbf{R}),$$

which provides  $C_{q\sigma} = \frac{w_{q\sigma}}{2c\beta_{q\sigma}}$  [90]. One can then write the field  $\mathbf{D}(\mathbf{R})$  in terms of the new photon eigenmode operators  $D_{\mathbf{q}\pm}$ , and replace it in the light-matter coupling Hamiltonian  $H_{\text{mat-pt}} = -\frac{1}{\epsilon_0} \int d\mathbf{R} \mathbf{P}(\mathbf{R}) \cdot \mathbf{D}(\mathbf{R})$ . Together with Eq. (3) of the main text, we obtain:

$$\begin{aligned} H_{\text{mat-pt}} &= -\hbar \omega_{\text{pl}} \sqrt{\frac{2c}{\tilde{\omega}_j \ell}} \sum_{\mathbf{Q}} \left\{ D_{\mathbf{q}+} \left[ iq \left( \Pi_{-\mathbf{Q}jz} + \Pi_{\mathbf{Q}jz}^\dagger \right) \mathcal{F}_+(Q) + \gamma_{\text{cr}} \left( \Pi_{-\mathbf{Q}j\parallel} + \Pi_{\mathbf{Q}j\parallel}^\dagger \right) \mathcal{F}_-(Q) \right] \right. \\ &\quad \left. - D_{\mathbf{q}-} \left[ iq \left( \Pi_{-\mathbf{Q}jz} + \Pi_{\mathbf{Q}jz}^\dagger \right) \mathcal{F}_-(Q) + \gamma_{\text{cr}} \left( \Pi_{-\mathbf{Q}j\parallel} + \Pi_{\mathbf{Q}j\parallel}^\dagger \right) \mathcal{F}_+(Q) \right] \right\} \quad (19) \end{aligned}$$

after spatial integration. The function  $\mathcal{F}_\pm(Q)$  stems from the overlap between the displacement and the polarization fields and reads  $\mathcal{F}_\pm(Q) = (\mathcal{F}_2(Q) \pm \mathcal{F}_1(Q))/\sqrt{2}$  with:

$$\mathcal{F}_1(Q) = e^{-\gamma_{\text{cr}}\ell} \left( \frac{1 - e^{-(iq_z - \gamma_{\text{cr}})\ell}}{iq_z - \gamma_{\text{cr}}} \right) \quad \mathcal{F}_2(Q) = \frac{1 - e^{-(iq_z + \gamma_{\text{cr}})\ell}}{iq_z + \gamma_{\text{cr}}}.$$

We now introduce the quasi-2D ‘‘bright’’ modes  $\pi_{\mathbf{q}\sigma j}^\dagger = \sum_{q_z, \alpha} f_{\alpha\sigma}(Q) \Pi_{\mathbf{Q}j\alpha}^\dagger$  and its hermitian conjugate, which consist of linear superpositions of the 3D plasmon-phonon hybrid modes with different  $q_z$ , and where  $f_{\alpha\sigma}(Q)$  reads:

$$f_{z\pm}(Q) = iq\mathcal{N}_{q\pm}\mathcal{F}_\pm(Q) \quad f_{//\pm}(Q) = \gamma_{\text{cr}}\mathcal{N}_{q\pm}\mathcal{F}_\mp(Q).$$

The normalization constant  $\mathcal{N}_{q\sigma}$  is determined by imposing the bosonic commutation relations  $[\pi_{\mathbf{q}\sigma j}, \pi_{\mathbf{q}'\sigma' j'}^\dagger] = \delta_{\mathbf{q}, \mathbf{q}'}$ , which provides  $1/\mathcal{N}_{q\pm}^2 = \sum_{q_z} q^2 |\mathcal{F}_\pm(q_z)|^2 + \gamma_{\text{cr}}^2 |\mathcal{F}_\mp(q_z)|^2$ . Transforming the summation into an integral  $\sum_{q_z} \rightarrow \ell/(2\pi) \int_{-\infty}^{+\infty} dq_z$ , and using the results:

$$\int dq_z |\mathcal{F}_m(Q)|^2 = \frac{\pi(1 - e^{-2\gamma_{\text{cr}}\ell})}{\gamma_{\text{cr}}} \quad \text{for } m = 1, 2, \quad \int dq_z \frac{e^{iq_z\ell}}{(iq_z + \gamma_{\text{cr}})^2} = \int dq_z \frac{e^{-iq_z\ell}}{(iq_z - \gamma_{\text{cr}})^2} = 2\pi\ell e^{-\gamma_{\text{cr}}\ell}, \quad (20)$$

and

$$\int dq_z \frac{e^{iq_z\ell}}{(iq_z - \gamma_{\text{cr}})^2} = \int dq_z \frac{e^{-iq_z\ell}}{(iq_z + \gamma_{\text{cr}})^2} = \int \frac{dq_z}{(iq_z \pm \gamma_{\text{cr}})^2} = 0, \quad (21)$$

we finally obtain:

$$\frac{1}{\mathcal{N}_{q\sigma}^2} = \frac{\ell}{2} \left[ \frac{q^2 + \gamma_{\text{cr}}^2}{\gamma_{\text{cr}}} (1 - e^{-2\gamma_{\text{cr}}\ell}) + 2\ell\sigma e^{-\gamma_{\text{cr}}\ell} (q^2 - \gamma_{\text{cr}}^2) \right]. \quad (22)$$

Note that the existence of a symmetry plane at  $z = \ell/2$  implies that the symmetric and antisymmetric bright modes commute, i.e.  $[\pi_{\mathbf{q}\sigma j}, \pi_{\mathbf{q}'\sigma' j'}^\dagger] = \delta_{\mathbf{q}, \mathbf{q}'} \delta_{\sigma, \sigma'} \delta_{j, j'}$ , which can be checked using Eqs. (20) and (21). On the other hand, the commutation relation with respect to  $j$  follows directly from the diagonalization of the matter Hamiltonian presented in the first section. One can then use Eq. (22) combined with the definition of the bright modes to write the light-matter coupling Hamiltonian Eq. (19) in the form given by Eq. (4) of the main text.

The total Hamiltonian Eq. (4) of the main text can be diagonalized numerically using a Hopfield-Bogoliubov transformation [105], namely by introducing the polariton eigenmodes of the system on the form:

$$\mathcal{P}_{\mathbf{q}\sigma\zeta} = \sum_{j=1,2} \left( O_{q\sigma j\zeta} \pi_{\mathbf{q}\sigma j} + \tilde{O}_{q\sigma j\zeta} \pi_{-\mathbf{q}\sigma j}^\dagger \right) + X_{q\sigma\zeta} D_{\mathbf{q}\sigma} + Y_{q\sigma\zeta} H_{\mathbf{q}\sigma}, \quad (23)$$

together with the condition  $[\mathcal{P}_{\mathbf{q}\sigma\zeta}, H] = w_{q\sigma\zeta} \mathcal{P}_{\mathbf{q}\sigma\zeta}$ . Computing this commutator, one can easily show that the polariton frequencies  $w_{q\sigma\zeta}$  in each subspace  $(\mathbf{q}, \sigma)$  are given by the 3 positive eigenvalues of the matrix:

$$\mathcal{H}_{\mathbf{q}\sigma} = \begin{bmatrix} \tilde{\omega}_1 & 0 & 0 & 0 & 0 & i\Omega_{q\sigma 1} C_{q\sigma} \\ 0 & -\tilde{\omega}_1 & 0 & 0 & 0 & i\Omega_{q\sigma 1} C_{q\sigma} \\ 0 & 0 & \tilde{\omega}_2 & 0 & 0 & i\Omega_{q\sigma 2} C_{q\sigma} \\ 0 & 0 & 0 & -\tilde{\omega}_2 & 0 & i\Omega_{q\sigma 2} C_{q\sigma} \\ \Omega_{q\sigma 1} & -\Omega_{q\sigma 1} & \Omega_{q\sigma 2} & -\Omega_{q\sigma 2} & 0 & 2ic\alpha_{q\sigma} C_{q\sigma} \\ 0 & 0 & 0 & 0 & -2ic\beta_{q\sigma} C_{q\sigma} & 0. \end{bmatrix} \quad (24)$$

Out of these three eigenvalues, only the lowest two correspond to surface modes as located below the light cone. These two surface modes are denoted as lower and upper polaritons with frequencies  $w_{q\sigma\text{LP}}$  and  $w_{q\sigma\text{UP}}$ , respectively. In order to compute these frequencies, we use a self-consistent algorithm which consists in starting with a given frequency  $w_{q\sigma\text{LP}}$ , then determine the penetration depths in each media from the Helmholtz equation  $\epsilon_n(w_{q\sigma\text{LP}})w_{q\sigma\text{LP}}^2/c^2 =$

$q^2 - \gamma_n^2$  with  $\epsilon_d = 1$  and  $\epsilon_{cr}$  given by Eq. (13), and use the values of  $\gamma_n$  to compute the parameters entering the matrix Eq. (24). The latter is diagonalized numerically allowing to determine the new  $w_{q\sigma LP}$ , and the whole process is repeated until convergence is reached. This method is applied independently for the symmetric and the antisymmetric modes  $\sigma = \pm$ .

The photon, phonon and plasmon weights of the polariton modes plotted on Fig. 2 are directly related to the transformation coefficients entering Eq. (23). From the polariton normalization:

$$\sum_{j=1,2} \left( |O_{q\sigma j\zeta}|^2 - |\tilde{O}_{q\sigma j\zeta}|^2 \right) - 2iC_{q\sigma} X_{q\sigma\zeta} Y_{q\sigma\zeta}^* = 1,$$

the photon weight is defined as  $W_{pt,q\sigma}^\zeta = -2iC_{q\sigma} X_{q\sigma\zeta} Y_{q\sigma\zeta}^*$ , and we now need to compute the phonon and plasmon weights of the hybrid plasmon-phonon modes  $j = 1, 2$ . This can be done by realizing that the frequencies  $\tilde{\omega}_1$  and  $\tilde{\omega}_2$  given by Eq. (1) of the main text are the eigenvalues of the effective plasmon-phonon coupling Hamiltonian  $H_{\text{eff}} = \hbar\omega_{pl} P^\dagger P + \hbar\tilde{\omega}_0 B^\dagger B + \hbar\Omega (P + P^\dagger) (B + B^\dagger)$ , where  $P$  and  $B$  denote respectively the effective plasmon and phonon bosonic operators,  $\Omega = (\nu_{pn}/2)\sqrt{\omega_{pl}/\tilde{\omega}_0}$  the effective coupling strength, and  $\tilde{\omega}_0^2 = \omega_0^2 + \nu_{pn}^2$  the renormalized phonon frequency. Introducing the normal modes  $\mathcal{P}_j^0 = U_j P + \tilde{U}_j P^\dagger + V_j B + \tilde{V}_j B^\dagger$  with the condition  $[\mathcal{P}_j^0, H_{\text{eff}}] = \tilde{\omega}_j \mathcal{P}_j^0$ , the coefficients  $U_j, \tilde{U}_j, V_j$ , and  $\tilde{V}_j$  can be computed similarly as before by diagonalizing the associated Hopfield matrix. Using the normalization condition  $|U_j|^2 - |\tilde{U}_j|^2 + |V_j|^2 - |\tilde{V}_j|^2 = 1$ , the phonon and plasmon weights of the polariton  $\zeta$  are defined as:

$$W_{pl,q\sigma}^\zeta = \sum_j \left( |U_j|^2 - |\tilde{U}_j|^2 \right) \left( |O_{q\sigma j\zeta}|^2 - |\tilde{O}_{q\sigma j\zeta}|^2 \right)$$

$$W_{pn,q\sigma}^\zeta = \sum_j \left( |V_j|^2 - |\tilde{V}_j|^2 \right) \left( |O_{q\sigma j\zeta}|^2 - |\tilde{O}_{q\sigma j\zeta}|^2 \right),$$

with  $\sum_i W_{i,q\sigma}^\zeta = 1$  ( $i = pt, pl, pn$ ).

### Effective quantum model in the vibrational ultrastrong coupling regime

We consider a metal-dielectric interface featuring a plasmon mode with plasma frequency  $\omega_m$  in the metal region, and a collection of vibrating ions with frequency  $\omega_0$  forming a lattice embedded in the dielectric region of permittivity 1 (e.g. air). Phonons are polarized in the directions  $\mathbf{u}_z$  and  $\mathbf{u}_\parallel = \mathbf{r}/r$ , and both metal and dielectric extend to infinity on each side. In the effective quantum model of Refs. [20 and 21], the PZW Hamiltonian of the system reads  $H = H_{\text{spp}} + H_{\text{pn-spp}} + H_{\text{pn}} + H_{\text{P}^2}$ , where  $H_{\text{spp}}$  is the effective SPP Hamiltonian,  $H_{\text{pn-spp}}$  is the SPP-phonon coupling, and  $H_{\text{pn}} = \sum_{\mathbf{Q},\alpha} \hbar\omega_0 B_{\mathbf{Q},\alpha}^\dagger B_{\mathbf{Q},\alpha}$  is the phonon Hamiltonian of the first section. Since there is no plasmon in the dielectric region, the term proportional to the square polarization reads  $H_{\text{P}^2} = \frac{1}{2\epsilon_0} \int d\mathbf{R} \mathbf{P}_{\text{pn}}^2(\mathbf{R})$ , where the phonon polarization field  $\mathbf{P}_{\text{pn}}$  is given by Eq. (7). As a particular case of the results presented in the first section, it is easy to show that the total phonon contribution to the Hamiltonian can be put in the diagonal form  $H_{\text{pn}} + H_{\text{P}^2} = \hbar\tilde{\omega}_0 \sum_{\mathbf{Q},\alpha} \tilde{B}_{\mathbf{Q},\alpha}^\dagger \tilde{B}_{\mathbf{Q},\alpha}$ , with the transformation:

$$B_{\mathbf{Q},\alpha} = \frac{\tilde{\omega}_0 + \omega_0}{2\sqrt{\omega_0\tilde{\omega}_0}} \tilde{B}_{\mathbf{Q},\alpha} - \frac{\tilde{\omega}_0 - \omega_0}{2\sqrt{\omega_0\tilde{\omega}_0}} \tilde{B}_{-\mathbf{Q},\alpha}^\dagger \quad B_{-\mathbf{Q},\alpha}^\dagger = -\frac{\tilde{\omega}_0 - \omega_0}{2\sqrt{\omega_0\tilde{\omega}_0}} \tilde{B}_{\mathbf{Q},\alpha} + \frac{\tilde{\omega}_0 + \omega_0}{2\sqrt{\omega_0\tilde{\omega}_0}} \tilde{B}_{-\mathbf{Q},\alpha}^\dagger. \quad (25)$$

Here, the renormalized phonon frequency is defined as  $\tilde{\omega}_0^2 = \omega_0^2 + \nu_{pn}^2$ , with  $\nu_{pn}$  the ionic plasma frequency (see main text). In the PZW representation, the effective SPP Hamiltonian reads:

$$H_{\text{spp}} = \frac{1}{2\epsilon_0} \int d\mathbf{R} \mathbf{D}^2(\mathbf{R}) + \frac{1}{2\epsilon_0 c^2} \int d\mathbf{R} \mathbf{H}^2(\mathbf{R}).$$

In stark contrast to the full quantum description of the previous sections, here, the displacement and magnetic fields  $\mathbf{D}$  and  $\mathbf{H}$  contain the contribution of the plasmon polarization and do not involve pure photonic degrees of freedom. The displacement field can be written as:

$$\mathbf{D}(\mathbf{R}) = i \sum_{\mathbf{q}} \sqrt{\frac{\epsilon_0 \hbar \xi_q}{2SL_{\text{eff}}(\xi_q)}} (a_{\mathbf{q}} - a_{-\mathbf{q}}^\dagger) \mathbf{U}_q e^{i\mathbf{q}\cdot\mathbf{r}}, \quad (26)$$

with  $S$  an arbitrary (large) surface in the plane, and  $a_{\mathbf{q}}$  and  $a_{\mathbf{q}}^\dagger$  the annihilation and creation operators of a SPP with frequency  $\xi_q$ , which satisfy the bosonic commutation relations  $[a_{\mathbf{q}}, a_{\mathbf{q}'}^\dagger] = \delta_{\mathbf{q}, \mathbf{q}'}$ . The mode functions read:

$$\mathbf{U}_q = \left( \mathbf{u}_{//} - \frac{q}{\gamma_d} \mathbf{u}_z \right) e^{-\gamma_d z},$$

and the penetration depths in the metal and dielectric regions  $\gamma_m$  and  $\gamma_d$  are related to the SPP frequency via the Helmholtz equation, namely  $\gamma_m = \sqrt{q^2 - \epsilon_m(\xi_q)\xi_q^2/c^2}$  and  $\gamma_d = \sqrt{q^2 - \xi_q^2/c^2}$ . The SPP frequency  $\omega = \xi_q$  is solution of the equation:

$$\omega = qc \sqrt{\frac{\epsilon_m(\omega) + 1}{\epsilon_m(\omega)}},$$

and  $\epsilon_m(\omega) = 1 - (\omega_m/\omega)^2$  is the Drude permittivity of the (lossless) metal. According to the SPP quantization scheme detailed in Refs. [57, 59, 72–74], the effective quantization length  $L_{\text{eff}}(\omega)$  is defined as:

$$2L_{\text{eff}}(\omega) = \frac{1}{2\gamma_m} \left[ \left( 1 + \frac{q^2}{\gamma_m^2} \right) \frac{d[\omega\epsilon_m(\omega)]}{d\omega} + \left| \frac{\epsilon_m(\omega)}{\gamma_m} \right|^2 \frac{\omega^2}{c^2} \right] + \frac{1}{2\gamma_d} \left[ \left( 1 + \frac{q^2}{\gamma_d^2} \right) + \frac{1}{|\gamma_d|^2} \frac{\omega^2}{c^2} \right].$$

With these definitions, one can show [57, 59, 72–74] that the effective SPP Hamiltonian takes the usual quantized form  $H_{\text{spp}} = \sum_{\mathbf{q}} \xi_q a_{\mathbf{q}}^\dagger a_{\mathbf{q}}$ . The phonon-SPP coupling Hamiltonian reads  $H_{\text{ph-spp}} = -\frac{1}{\epsilon_0} \int d\mathbf{R} \mathbf{P}_{\text{pn}}(\mathbf{R}) \cdot \mathbf{D}(\mathbf{R})$ . We express the phonon polarization field  $\mathbf{P}_{\text{pn}}$  Eq. (7) in terms of the new operators  $\tilde{B}_{\mathbf{Q},\alpha}$  and  $\tilde{B}_{-\mathbf{Q},\alpha}^\dagger$  defined by Eq. (25), and use the expression of the displacement field Eq. (26). The phonon-SPP coupling can be put in the form:

$$H_{\text{ph-spp}} = \sum_{\mathbf{q}} i\hbar\Omega_q (b_{-\mathbf{q}} + b_{\mathbf{q}}^\dagger) (a_{\mathbf{q}} - a_{-\mathbf{q}}^\dagger),$$

with the vacuum Rabi frequency:

$$\Omega_q = \nu_{\text{pn}} \sqrt{\frac{\xi_q}{8\tilde{\omega}_0 L_{\text{eff}}(\xi_q) \gamma_d}} \sqrt{1 + \frac{q^2}{\gamma_d^2}}.$$

Similarly as in the previous section, the quasi-2D phonon operators are defined as:

$$b_{\mathbf{q}} = \mathcal{N}_q \sum_{q_z} \frac{(q/\gamma_d) \tilde{B}_{\mathbf{Q},z} - \tilde{B}_{\mathbf{Q},//}}{\gamma_d - iq_z},$$

where the normalization  $\mathcal{N}_q$  is determined by the bosonic commutation relation  $[b_{\mathbf{q}}, b_{\mathbf{q}}^\dagger] = 1$ , which provides  $\frac{1}{\mathcal{N}_q^2} = \sum_{q_z} \frac{1+(q/\gamma_d)^2}{\gamma_d^2+q_z^2}$ . Gathering the different contributions, the effective quasi-2D Hamiltonian reads:

$$H = \sum_{\mathbf{q}} \hbar\xi_q a_{\mathbf{q}}^\dagger a_{\mathbf{q}} + \sum_{\mathbf{q}} i\hbar\Omega_q (b_{-\mathbf{q}} + b_{\mathbf{q}}^\dagger) (a_{\mathbf{q}} - a_{-\mathbf{q}}^\dagger) + \hbar\tilde{\omega}_0 \sum_{\mathbf{q}} b_{\mathbf{q}}^\dagger b_{\mathbf{q}},$$

and can be diagonalized using a Hopfield-Bogoliubov transformation. The two resulting polaritons modes are represented on Fig. 3 for  $\nu_{\text{pn}} = 0.01\omega_0$  (dotted lines),  $\nu_{\text{pn}} = 0.5\omega_0$  (dashed lines), and  $\nu_{\text{pn}} = \omega_0$  (solid lines). The lower  $\zeta = \text{LP}$  and upper  $\zeta = \text{UP}$  polaritons are depicted as red and blue lines, respectively. While the limiting behaviors of the LP  $w_{q\text{LP}} \sim qc$  for  $q \rightarrow 0$  and the UP  $w_{q\text{UP}} \rightarrow \omega_m/\sqrt{2}$  for  $q \rightarrow \infty$  are properly described by the model,  $w_{q\text{UP}}$  for  $q \rightarrow 0$  and  $w_{q\text{LP}}$  for  $q \rightarrow \infty$  feature unphysical behaviors in the ultrastrong coupling regime, i.e. when  $\nu_{\text{pn}}$  is a non-negligible fraction of  $\omega_0$ . Indeed,  $w_{q\text{LP}}$  exhibits irregularities in the regime of large detunings  $q \gg q_0$  (see inset), and becomes larger than  $\omega_0$  while increasing the coupling strength  $\nu_{\text{pn}}$ . We conclude that the effective quantum model based on quantized SPPs is well suited as long as the coupling strength does not exceed a few percent of the associated transition frequency, and therefore fails in the ultrastrong coupling regime.

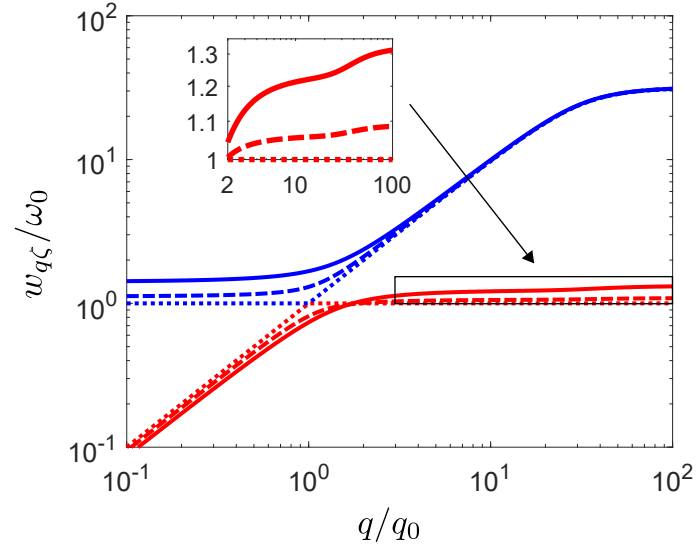


FIG. 3. Log-log scale: Normalized polariton frequencies  $w_{q\zeta}/\omega_0$  versus in-plane wave vector  $q/q_0$  ( $q_0 = \omega_0/c$ ), for  $\nu_{pn} = 0.01\omega_0$  (dotted lines),  $\nu_{pn} = 0.5\omega_0$  (dashed lines), and  $\nu_{pn} = \omega_0$  (solid lines). The lower  $\zeta = \text{LP}$  and upper  $\zeta = \text{UP}$  polaritons are depicted as red and blue lines. The region delimited by the rectangle is magnified in the inset. The plasma frequency is chosen as  $\omega_m = 45\omega_0$ , which corresponds to  $\hbar\omega_m = 9\text{eV}$  (gold or silver) for  $\hbar\omega_0 = 200\text{meV}$  (mid-infrared optical phonons).